

Evaluation of blast impact pressure by artificial joint condition using numerical analysis

You-Song Noh^{*}, Hoon Park^{**†}, and Chul-Gi Suk^{*}

^{*}Korea Kacoh Co., Ltd., 334-1 Digital-ro, Yeongdeungpo-gu, Seoul, 07448, REPUBLIC OF KOREA

[†]Corresponding author: hujin@jbnu.ac.kr

Phone: +82-2-834-4590

^{**}Chonbuk National University, 567 Baekje-daero, Deokjin-gu, Jeonju-si, Jeollabuk-do, 54896, REPUBLIC OF KOREA

Received: November 3, 2017 Accepted: October 2, 2019

Abstract

This study undertakes an evaluation of blast impact effect through the analysis of the contribution rate and effect that different artificial joint number, artificial joint spacing, and artificial joint angle have on blast velocity and pressure. Blast velocity and pressure according to the different state of the artificial joint was obtained using AUTODYN, a dynamic analysis program. The result of the numerical analysis was subject to further normalization analysis. For the contribution rate of design factors was analyzed using the robust design method. The orthogonal array used in the analysis was $L_9(3^1)$, and the parameters were artificial joint number, artificial joint spacing and artificial joint angle for each parameter having 3 levels. The result of normalization analysis regarding the numerical analysis was indicated a tendency in which blast velocity decreased and blast pressure increased as joint angle increased. The result of analyzing blast pressure and velocity regarding joint spacing and joint angle was indicated a tendency in which blast velocity decreased as joint spacing increased when the angle was perpendicular and blast pressure was decreased as the more increasing joint spacing at the all joint angle parameters. The result of the contribution rate analysis using robust design was indicated that artificial joint angle had the largest effect on blast velocity, followed by artificial joint numbers and the artificial joint spacing. In the case of blast pressure contribution rates, they were ranked in the descending order of artificial joint angle, artificial joint numbers, and artificial joint spacing.

Keywords: artificial joint, robust design, AUTODYN, blast velocity, blast pressure

1. Introduction

Due to the effect of urbanization, for the efficient use of limited space of city area has led to the development of underground social infrastructure. Also, there has been increasing demand for underground space and underground traffic routes. However, the high cost of undertaking construction underground in urban center as well as the vibration, noise, possible fracturing of neighboring buildings, ground subsidence, and civil complaints associated with the construction process raise various problems. Currently, blast method based on explosive used to secure underground space was considered to be the most effective in terms of economy and ease of construction¹⁾, but blast method inevitably raise issues of vibration and noise. Such forms of blast pollution are largely limiting the process of undertaking

blast work²⁾. As a means of remedying such forms of blast pollution, methods such as smooth blasting and controlled blasting have recently been used³⁾. When continual artificial free face exist, seismic waves such as blast vibration was not transmitted beyond the artificial free face and was captured within the artificial free face^{4), 5)}. This principle has been applied for use to undertake blast work in which an artificial free face was shaped using an abrasive material water jet system and wire-saw method⁵⁾⁻⁸⁾.

In this study, we conducted the analysis of the blast velocity and pressure that occur during single hole blasting activities for the purpose of applying artificial joint to tunnel excavation. The design of each numerical analysis was used method of design of experiment. The numerical analyses were conducted about the various

Table 1 Various orthogonal arrays.

Orthogonal Array	Total case	Actual case	Remarks
L ₄ (2 ³)	8	4	2 levels 3 parameters
L ₈ (2 ⁷)	128	8	2 levels 7 parameters
L ₉ (3 ⁴)	80	9	3 levels 4 parameters
L ₁₂ (2 ¹¹)	2,048	12	2 levels 11 parameters
L ₁₆ (2 ¹⁵)	32,768	16	2 levels 15 parameters
L ₁₆ (4 ⁵)	1,024	16	4 levels 5 parameters
L ₁₈ (2 ¹ × 3 ⁷)	4,374	18	2 and 3 levels 8 parameters
L ₂₅ (5 ⁶)	15,625	25	5 levels 6 parameters
L ₂₇ (3 ¹³)	1,594,324	27	3 levels 13 parameters
L ₃₂ , L ₃₆ , L ₅₀ etc.			etc.

artificial joint conditions and the blast velocity and pressure were calculated at the same point. The contribution rate of the different artificial joint parameter was evaluated by ranking the measurement values according to the robust design.

2. Parameter design

2.1 Design of experiment

For the purpose of evaluating the effect and contribution rate of the parameters, the robust design was used. The robust design involves the undertaking of experiments independently, a limited number of times, according to the values of an array in which the method produces the same effect as undertaking an immensely large number of experiments. Table 1 presents an orthogonal array that is typically used.

The L₈ (2⁷) orthogonal array of Table 1 presents 2 levels, or in other words, a situation where there are 7 selectable parameters in which two need to be selected. In this case, the total experiments were 128 cases. But we were expected to obtain same result of data for total experiment case through conducted only 8 experiments. And the optimal conditions in which the parameters reciprocally interact can be ascertained. The individual effect and optimization of each parameter can be found using analysis of means (ANOM) and the relative effects and sensitivities of the parameters can be obtained using analysis of variance (ANOVA). The adopted optimal statistical volumes for such analyses were defined as Equation 1. This was referred to as the SN ratio.

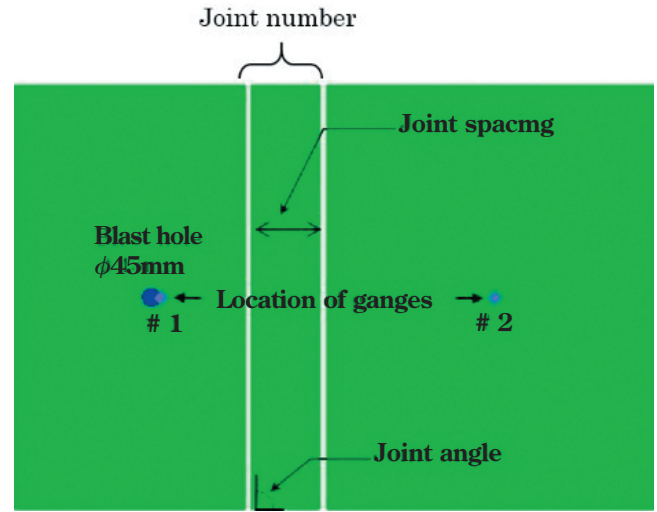
$$SNratio = -10 \cdot \log \left(\frac{1}{n} \cdot \sum_{i=1}^n Y_i^2 \right) \quad (1)$$

Where, n is the number of measured values, and Y_i is the measured feature value.

The effect of the parameter level is defined as the deviation of the parameter level results from the total average⁹⁾.

2.2 Establishment of design parameters

For the purpose of undertaking contribution rate analysis regarding blast velocity and pressure based on multiple artificial joints, the selected parameters, as presented in Figure 1, including the artificial joint numbers, the artificial joint spacing, and the artificial joint

**Figure 1** Parameter model of numerical analysis.**Table 2** Orthogonal array L₉ (3⁴).

No.	Parameter A	Parameter B	Parameter C	Parameter D
1	1	1	1	1
2	1	2	2	2
3	1	3	3	3
4	2	1	2	3
5	2	2	3	1
6	2	3	1	2
7	3	1	3	2
8	3	2	1	3
9	3	3	2	1

angle.

The experiment design was set to have 3 levels for each parameter and thus a 3 level 3 parameters orthogonal array L₉ (3⁴) was selected. Table 2 shows the orthogonal array L₉ (3⁴).

Table 3 shows the parameter levels. Where A was the artificial joint number, B was the artificial joint spacing, and C was the artificial joint angle. The artificial joint spacing was set as 5, 10, and 15 times the 11 mm spacing of the wire saw cutting surface area.

The characteristics for the contribution rate analysis were calculated through numerical analysis and blast velocity and pressure were selected as the characteristics.

Table 3 Three levels of design parameters.

Level	Artificial joint number (A) [ea]	Artificial joint spacing (B) [mm]	Artificial joint angle (C) [°]
Level 1	2	55	45
Level 2	3	110	60
Level 3	4	165	90

3. Numerical analysis

3.1 Applied physical properties

The RHT (Reidel-Hermaier-Thoma) concrete model established by Riedel et al.¹⁰⁾ was a model used to analyze general brittle material. The RHT concrete model was used as the physical property model for brittle material in dynamic analysis programs such as AUTODYN and LS-DYNA. The RHT model was especially useful for the modeling of concrete subject to dynamic loads. It was also used to model other materials brittle material such as rock and ceramics. And it also considered the effect of shearing strength reduction, weakening of deformation rate due to damage, stiffening of deformation rate velocity, stiffening of deformation rate and stiffening of pressure. Table 4 presents the RHT model physical values applied in this study. Air was modeled into the joint area. To establish the atmospheric conditions of the air, internal energy was set to standard atmospheric conditions of 2.068×10^5 J·kg⁻¹, the ideal gas equation was used. The physical properties of the applied explosives were as presented in Table 5.

3.2 Analysis method and analysis result

For the numerical experiments, a total of 9 analyses were undertaken using AUTODYN 2D according to the conditions of the orthogonal array of Table 2. The rock area was formed using a Lagrange solver and the outer boundary of the rock area was set to have transmit boundary conditions to represent infinity. The size of the blast hole was set as $\phi 45$ mm, which is typically applied in actual tunnel sites.

The gauges were installed as shown in Figure 1 to obtain the data of blast velocity and pressure for all cases. The initial blast velocity and pressure were measured by installing a gauge 1 at the next node of the blast hole. The blast velocity and pressure used for robust design analysis were measured by gauge 2 in the equal location after passing through all joint area. The result of the measured initial blast velocity and pressure were 477.68 m·s⁻¹ and 3,529.6 MPa respectively, the all cases were obtained the equal result value. Figure 2 shows time history graphs of initial blast velocity and pressure of No. 3.

Numerical analysis indicated the development of reflected tensile waves once the blast pressure reached the artificial joint area (Figure 3a). Transmission of the blast pressure was found to have occurred during the analysis, after contact was made with the next rock element as the joint area closed (Figure 3b). Regarding the joint angle, blast pressure was transmitted first in the joint area at a perpendicular angle with the blast source. The reflected tensile wave and transmission of pressure were

Table 4 Parameters of the RHT model.

Parameter	Value
Reference density	2.75 [g·cm ⁻³]
Porous density	2.52 [g·cm ⁻³]
Porous sound speed	3.242×10^3 [m·s ⁻¹]
Initial compaction pressure	93.30 [MPa]
Solid compaction pressure	6.000×10^3 [MPa]
Compaction exponent	3.000
Bulk modulus, A_1	3.527×10^4 [MPa]
Bulk modulus, A_1	3.958×10 [MPa]
Parameter, A_3	9.040×10^2 [MPa]
Parameter, B_0	1.220
Parameter, B_1	1.220
Parameter, T_1	3.527×10^4 [MPa]
Parameter, T_2	0.000 [MPa]
Reference temperature	300 [K]
Specific heat	6.540×10^2 [J·kgK ⁻¹]
Thermal conductivity	0.000
Shear modulus, G	2.206×10^4 [MPa]
Compressive strength, f_c	93.75 [MPa]
Tensile strength, $f_t \cdot f_c^{-1}$	0.100
Shear strength, $f_s \cdot f_c^{-1}$	0.180
Intact failure surface constant, A	1.600
Intact failure surface exponent, N	0.610
Tens. · Comp. meridian ratio ⁻¹ , $Q_{2,0}$	6.805×10^{-1}
Brittle to ductile transition, BQ	1.050×10^{-2}
G (elastic) · G (elastic-plastic) ⁻¹	2.000
Elastic strength f_t^{-1}	0.700
Elastic strength f_c^{-1}	0.530
Residual strength constant, B	1.600
Residual strength exponent, M	0.610
Compressive strain rate exponent, α	9.090×10^{-3}
Compressive strain rate exponent, δ	1.250×10^{-2}
Max. fracture strength ratio	1.000×10^{20}

Table 5 Characteristics of explosives (JWL, C-J).

A [GPa]	B [GPa]	R_1	R_2	ω
49.46	1.891	3.907	1.118	0.333

occurred in that area (Figure 3).

Figures 4 and Figure 5 present graphs on the result of the joint angle and joint spacing regarding the normalization of blast velocity and pressure passing through one joint area and two joint areas. The analysis result indicated a tendency in which blast velocity

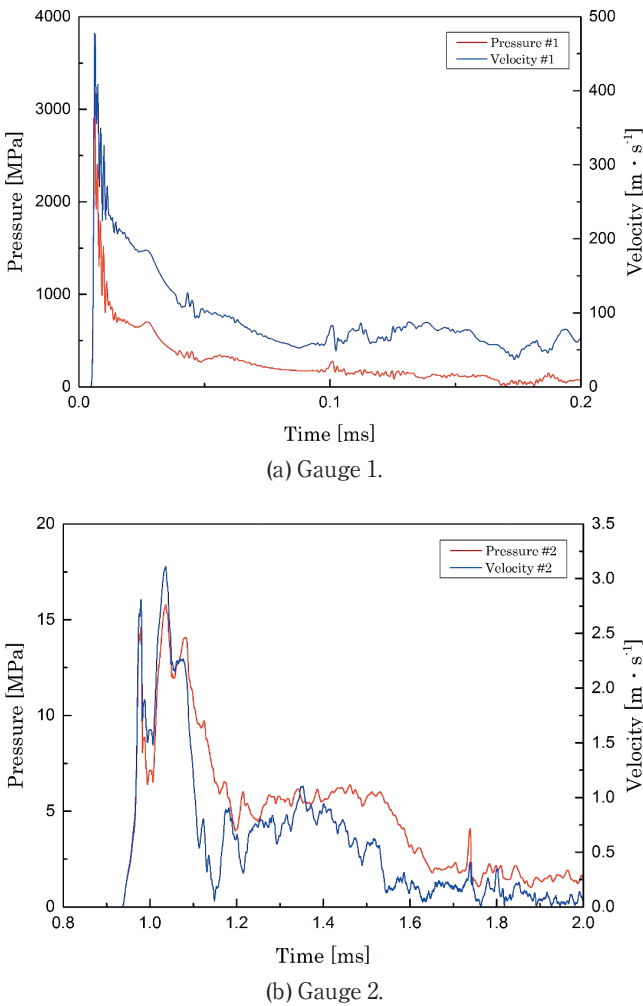


Figure 2 Time-history graph of initial blast velocity and pressure of No. 3.

decreased as joint angle increased while blast pressures showed a tendency of increasing (Figure 4). The result of analyzing blast velocity by joint spacing and joint angle indicated that when the joint angle was perpendicular, a tendency in which blast velocity decreased as joint spacing increased was presented. On the other hand, at 45° joint angle, blast velocity was found to decrease as joint spacing decreased. For 60° joint angle, blast velocity was found to decrease as joint spacing increased, yet blast velocity increased for joint spacing of 110 mm or greater. Blast pressure overall indicated a tendency to decrease as joint spacing increased (Figure 5).

The blast velocity and pressure measurement values to be used for ANOM and ANOVA were ascertained from the gauges in the same locations as presented in Figure 1 according to the numerical analysis of each case of analysis. The results were as presented in Table 6.

4. Results of analysis

The applied robust design method uncovers largely influential parameters that can be controlled and minimizes the effect of noise by maximizing the effects of such parameters. To maintain robustness of quality, SN ratio was used. The SN ratio means signal to noise ratio; it was indicated the ratio between the force of the inputted signal and the influence of noise. In other words, by

selecting parameter values that maximize the SN ratio; of each of the control parameters, the selected value can become robust against noise. The definition of SN ratios differs according to the objective function or the characteristics in which the characteristics are classified into the characteristics of normal is best, smaller is better, or larger is better¹¹⁾. The applied method in this study was smaller is better characteristic in which the smaller the blast velocity and pressure the better. The calculation was made using Equation 1 and the result was shown in Table 7.

To find the optimal level, ANOM and ANOVA were undertaken using the SN ratios of the blast velocity and pressure. As an example of ANOM, the average SN ratio of A parameter level 1 was calculated by averaging the SN ratio of number of experiment 1, 2, and 3. Using such method the effect of all parameter and level were calculated. Furthermore, in the case of ANOVA, calculation of the sum of the square of each parameter using Equation 2 was undertaken

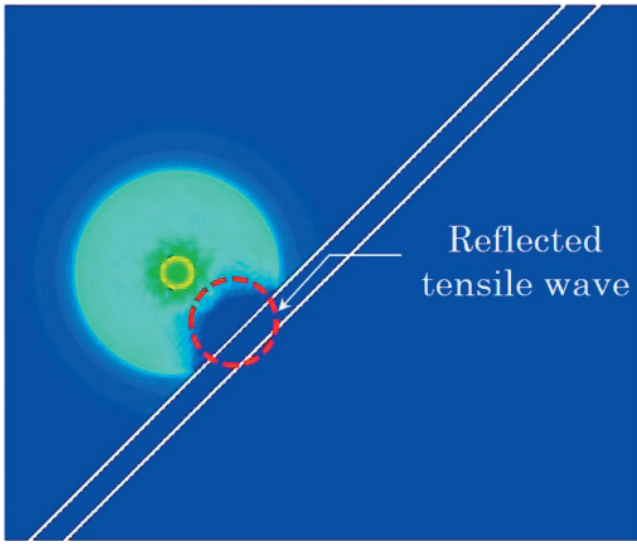
$$\text{Sum of Squares} = 3 \cdot (m_1 - m)^2 + 3 \cdot (m_2 - m)^2 + 3 \cdot (m_3 - m)^2 \quad (2)$$

Where, m is the total SN ratio average, m_{1-3} is the average SN ratio of each level of each parameter. The calculated sum of square values was divided by the degree of freedom of each parameter (level - 1) to find the square average. Using the total sum of square average and the square average ratio, the contribution rate of each parameter were evaluated. The analysis results of blast velocity and pressure were presented in Table 8 and Table 9.

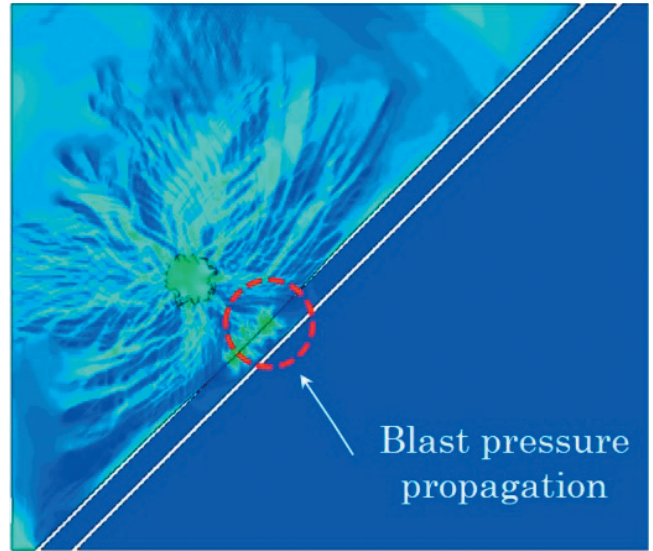
Figure 6 presents the SN ratio of each level of each parameter and the optimal parameter having minimal blast velocity was found to be A3B2C2 level in other words 4 joints, a joint spacing of 110 mm, and a joint angle of 60°. The optimal parameter having minimal blast pressure was found to be A3B2C1 in other words 4 joints, a joint spacing of 110 mm, and a joint angle of 60°. The result analyzing the contribution rates indicated that the parameter that affect blast velocity was ranked in the descending order of joint angle at 64.68 %, joint number at 31.05 %, and joint spacing at 4.27 %. The parameter that affect blast pressure was found to be ranked in the descending order of joint angle at 77.05 %, joint number at 18.59 %, and joint spacing at 4.36 %. The evaluation result indicated that the joint angle had the largest effect on blast velocity and pressure.

5. Conclusion

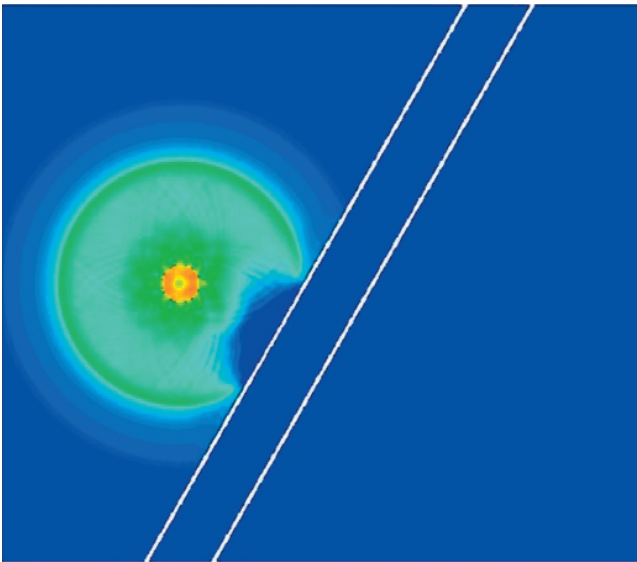
The effect of blast velocity and pressure according to different medium was numerically analyzed using AUTODYN. A robust design method was used to evaluate the optimal condition and contribution rate of each artificial joint parameter. The table of orthogonal arrays used in the analysis was $L_9(3^4)$, and the parameters to use analysis were artificial joint number, artificial joint spacing, and artificial joint angle – each parameters having 3 levels. Through ANOM and ANOVA, the



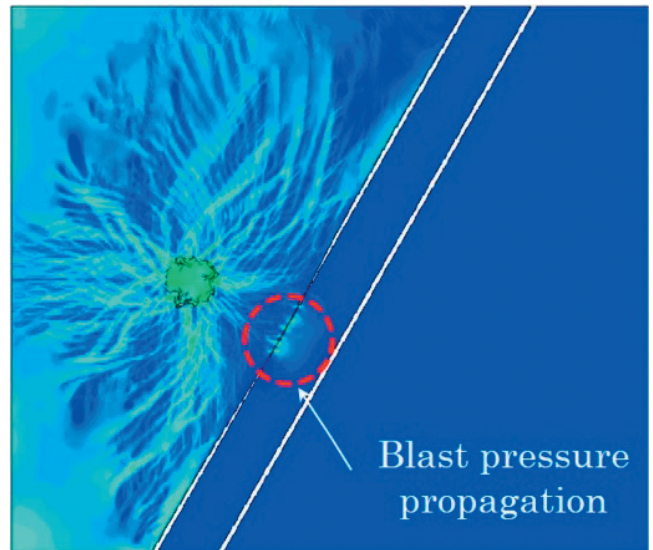
(a) Joint angle 45°.



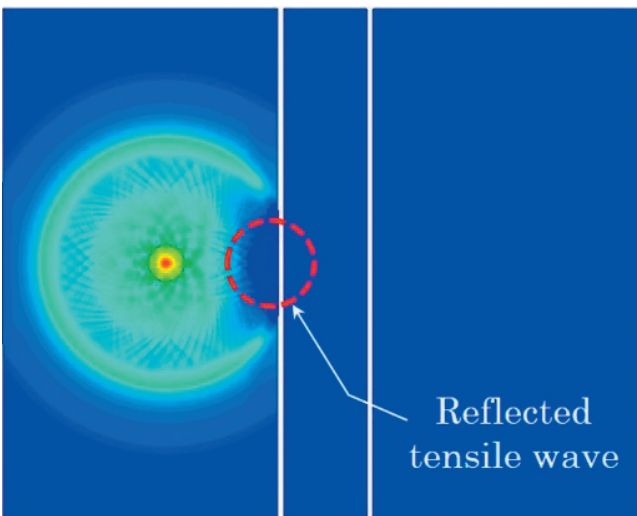
(b) Joint angle 45°.



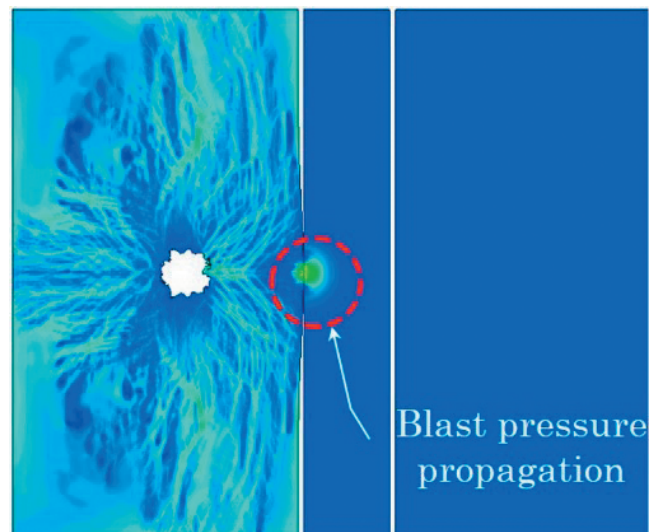
(c) Joint angle 60°.



(d) Joint angle 60°.



(e) Joint angle 90°.



(f) Joint angle 90°.

Figure 3 Occurrence of reflected tensile waves of each joint angle and propagation of blast pressure.

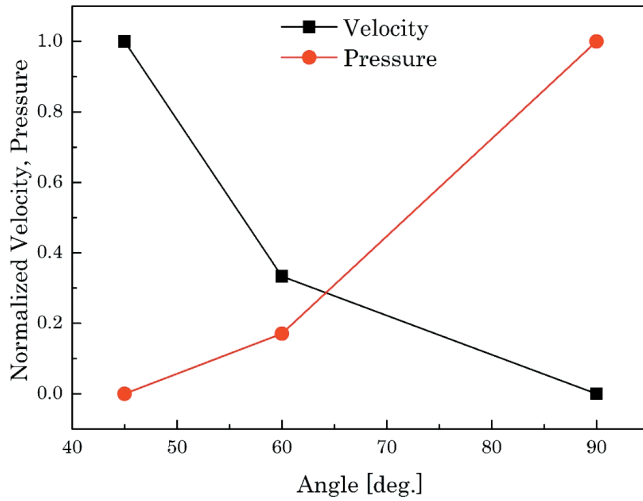


Figure 4 Result of normalization analysis passing one joint section.

following results were found.

(1) The result of numerical analysis through normalization analysis seemed to indicate that blast velocity decreased as joint angle increased yet showed a tendency for blast pressure to increase and the result of analyzing blast velocity according to joint spacing and angle indicated that, when the angle was perpendicular, blast velocity decreased as joint spacing increased. Also, the result of analyzing blast pressure indicated a tendency that revealed that, for all joint angles, blast pressures decrease as joint spacing increase.

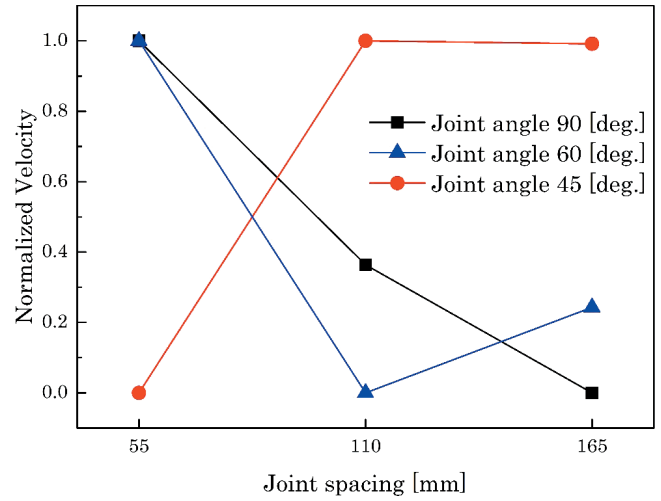
(2) The parameter that most largely affected blast velocity was found to be joint angle, followed by the parameters regarding the joint number and joint spacing.

(3) The optimal combination to minimize blast velocity was found to be 4 joints, a joint spacing of 110mm, and a joint angle of 60°.

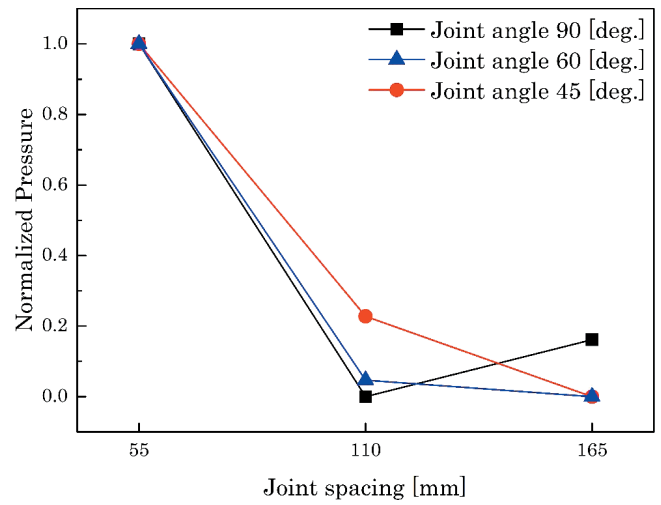
(4) The parameter that most largely affected blast pressure was found to be joint angle, followed by the parameters regarding the joint number and joint spacing.

(5) The optimal combination to minimize blast pressure was found to be 4 joints, a joint spacing of 110mm, and a joint angle of 45°.

(6) The joint angle was found to have the largest effect on blast velocity and blast pressure.



(a) Blast velocity.



(b) Blast pressure.

Figure 5 Result of normalization analysis passing two joint section.

Acknowledgements

This work was supported by a grant from the Korea Agency for Infrastructure Technology Advancement (KAIA) funded by the Ministry of Land, Infrastructure and Transport (Grant 17CTAP-C130130-01).

Table 6 Result of numerical analysis.

No.	<i>A</i> [ea]	<i>B</i> [mm]	<i>C</i> [°]	Max blast velocity [m·s ⁻¹]	Max blast pressure [MPa]
1	1	1	1	2.1030	9.3619
2	1	2	2	1.2994	6.3027
3	1	3	3	3.3555	18.2540
4	2	1	2	1.3952	5.6916
5	2	2	3	2.3690	15.33
6	2	3	1	1.0823	46.3970
7	3	1	3	1.8669	12.0009
8	3	2	1	1.0002	2.7884
9	3	3	2	1.0035	5.4351

Table 7 SN ratio of experimental result.

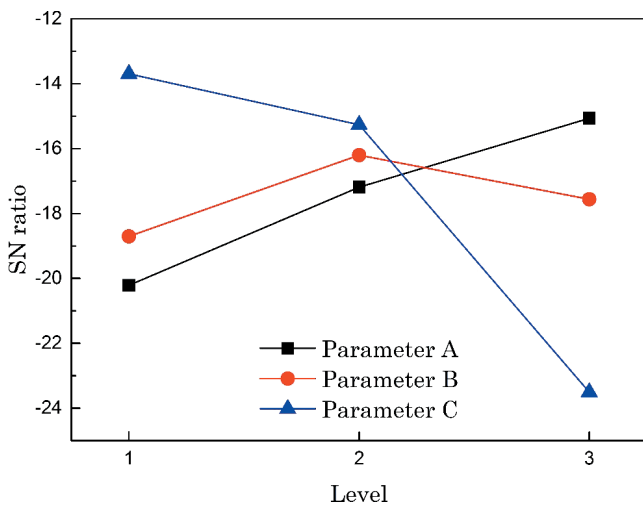
No.	A	B	C	Blast velocity SN ratio	Blast pressure SN ratio
1	1	1	1	-6.4570	-19.4273
2	1	2	2	-2.2749	-15.9905
3	1	3	3	-10.5151	-25.2272
4	2	1	2	-2.8927	-15.1047
5	2	2	3	-7.4913	-23.7108
6	2	3	1	-0.6870	-32.7492
7	3	1	3	-5.4224	-21.5843
8	3	2	1	-0.0017	-8.9071
9	3	3	2	-0.0304	-14.7042
Average				-3.9747	-17.4895

Table 8 Effect of parameter on blast velocity.

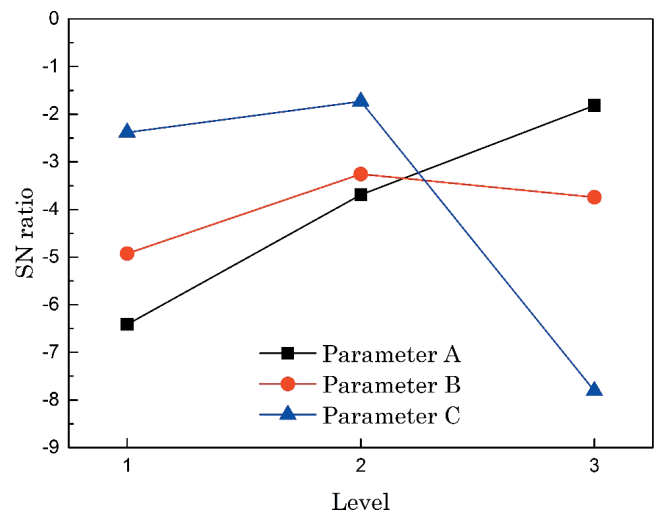
Parameter	Level 1	Level 2	Level 3	Deviation	DOF	Sum of square value	Square value average	Contribution rate [%]
A	-6.416	-3.690	-1.818	4.598	2	32.077	16.0385	31.05
B	-4.924	-3.256	-3.744	1.668	2	4.413	2.2065	4.27
C	-2.382	-1.733	-7.810	6.077	2	66.814	33.407	64.68

Table 9 Effect of parameter on blast pressure.

Parameter	Level 1	Level 2	Level 3	Deviation	DOF	Sum of square value	Square value average	Contribution rate [%]
A	-20.215	-17.188	-15.065	5.150	2	40.192	20.096	18.59
B	-18.705	-16.202	-17.560	2.053	2	9.420	4.710	4.36
C	-13.695	-15.267	-23.570	9.812	2	166.644	83.322	77.05



(a) Blast velocity.



(b) Blast pressure.

Figure 6 Main effects plot for SN ratio.

References

- 1) G. Berta, Tunnelling and Underground Space Technology, 9, 175–187 (1994).
- 2) H. S. Jung, K. S. Jung, H. N. Mun, B. S. Chun, and D. H. Park, Journal of Korean Geo-Environmental Society, 12, 5–14 (2011). (in Korean).
- 3) O. Uysal, K. Erarslan, M. A. Cebi, and H. Akcakoca, Journal of Rock Mechanics and Mining Science, 45, 712–719 (2008).
- 4) J. C. Santamarina, K. A. Klein, and M. A. Fam, “Soils and Waves”, Wiley, 448 (2001).
- 5) D. H. Park, B. K. Jeon, and S. W. Jeon, Rock Mechanics and Rock Engineering, 42, 449–473 (2009).
- 6) J. G. Kim, “Reduction of blasting-induced vibration in tunneling using abrasive water jet notch and disc cutting”, 340–341, Ph.D. Thesis, Seoul National University (2012). (in Korean).

- 7) T. M. Oh, G. C. Cho, and I. T. Ji, *Journal of Korean Tunneling and Underground Space Association*, 15, 49–57 (2013). (in Korean).
- 8) J. H. Lee, S. K. Ahn, K. C. Lee, C. S. Bang, and M. Sagong, *Transactions Korean Society of Mechanical Engineering A*, 37, 1069–1077 (2015). (in Korean).
- 9) H. S. Yang, *Explosive & Blasting*, 31, 1–5 (2013). (in Korean).
- 10) W. Riedel, K. Thomas, S. Hiermaier, and E. Schmolinske, *Proceedings of the 9th International Symposium on the Interaction of the Effects of Munitions with Structures*, 315–322, Germany (1999).
- 11) N. K. Baek and D. E. Kim, *Journal of the Korean Society of Precision Engineering*, 19, 59–63 (2002). (in Korean).